Journal of Agriculture and Food Research 18 (2024) 101362

Contents lists available at ScienceDirect

Journal of Agriculture and Food Research

journal homepage: www.sciencedirect.com/journal/journal-of-agriculture-and-food-research

Identification of novel functional compounds from forest onion and its biological activities against breast cancer

Fahrul Nurkolis [a], Isma Kurniatanty [a], Elvan Wiyarta [b], Happy Kurnia Permatasari [c], Nelly Mayulu [d], Nurpudji Astuti Taslim [e], Raymond Rubianto Tjandrawinata [f], Hardinsyah Hardinsyah [g], Trina Ekawati Tallei [h], Apollinaire Tsopmo [i], Son Radu [j], Edwin Hadinata [k], Bonglee Kim [l], Rosy Iara Maciel Azambuja Ribeiro [m], Rony Abdi Syahputra [n,*]

[a] Department of Biological Sciences, Faculty of Sciences and Technology, State Islamic University of Sunan Kalijaga (UIN Sunan Kalijaga), Yogyakarta, 55281, Indonesia
[b] Department of Neurology, Faculty of Medicine, Universitas Indonesia - Dr. Cipto Mangunkusumo National Hospital, Jakarta, 10430, Indonesia
[c] Department of Biochemistry and Biomolecular, Faculty of Medicine, University of Brawijaya, Malang, 65145, Indonesia
[d] Department of Nutrition, Faculty of Health Science, Muhammadiyah Manado University, Manado, 95249, Indonesia
[e] Division of Clinical Nutrition, Department of Nutrition, Faculty of Medicine, Hasanuddin University, Makassar, 90245, Indonesia
[f] Department of Biotechnology, Faculty of Biotechnology, Atma Jaya Catholic University of Indonesia, Jakarta, 12930, Indonesia
[g] Division of Applied Nutrition, Department of Community Nutrition, Faculty of Human Ecology, IPB University, West Java, Bogor, 16680, Indonesia
[h] Department of Biology, Faculty of Mathematics and Natural Sciences, Universitas Sam Ratulangi, Manado, 95115, Indonesia
[i] Food Science Program, Department of Chemistry, Institute of Biochemistry, Carleton University, 1125 Colonel by Drive, Ottawa, K1S 5B6, ON, Canada
[j] Department of Food Science, Faculty of Food Science and Technology, Universiti Putra Malaysia, Selangor, UPM Serdang, 43400, Malaysia
[k] Internal Medicine, Hermina Pasuruan Hospital, Pasuruan, 67181, East Java, Indonesia
[l] Department of Pathology, College of Korean Medicine, Kyung Hee University, Seou, 02447, Republic of Korea
[m] Experimental Pathology Laboratory, Midwest Campus, Federal University of São João del-Rei, Divinópolis, Brazil
[n] Department of Pharmacology, Faculty of Pharmacy, Universitas Sumatera Utara, Medan, 20155, Indonesia

ARTICLE INFO

Keywords:
Anticancer
Natural product
Functional food
Avenasterol
PARP1
MCF-7
Forest onion
Network pharmacology
Antioxidant capability

ABSTRACT

The discovery of new molecules from natural sources for the treatment of tumors such as breast cancers is of importance for the development of functional foods and to the pharmaceutical industry. A natural resource with potential activity against breast cancer is forest onion, *Eleutherine bulbosa* (Mill.) Urb., but the identity of its active constituents and their mechanisms of action remain unexplored. Therefore, this study focuses on metabolite profiling, *in silico* or pharmacoinformatic activity and mechanisms, as well as advanced validation on *in vitro* cell lines. Ten compounds identified in *E. bulbosa* bulb ethanolic extract (EBE) showed cancer receptor and radical inhibitory activity via network pharmacology and molecular docking simulation. The most promising compound was avenasterol binding PARP-1, HER2, iNOS receptors with values of −11.26, −8.34, and −9.17 μg/mL, respectively. EBE and avenasterol had a smaller EC_{50} value, or higher potency, than the control antioxidant Trolox in radical scavenging tests with ABTS and DPPH. In line with the *in silico* study, EBE and avenasterol showed antiproliferative activity against human breast cancer MCF-7 with LD_{50} 217.8 μg/mL, with relatively low cytotoxicity to normal MCF-10A cells ($LD_{50} > 1000$ μg/mL). The antiproliferative mechanism of EBE on MCF-7 was associated with downregulation of TGF-β, HER2, PI3K, and AKT which are known tumor activators. Significant ($p < 0.05$) upregulation of tumor suppressor gene miR-29a-3p in MCF-7 was observed after treatment with EBE in a dose-dependent manner.

* Corresponding author.
E-mail addresses: fahrul.nurkolis.mail@gmail.com, fahrul24001@mail.unpad.ac.id (F. Nurkolis), isma.kurniatanty@uin-suka.ac.id (I. Kurniatanty), elvan.wiyarta@ui.ac.id (E. Wiyarta), happykp@ub.ac.id (H.K. Permatasari), nmayulu@unsrat.ac.id (N. Mayulu), pudji_taslim@yahoo.com (N.A. Taslim), raytjan@yahoo.com (R.R. Tjandrawinata), hardinsyah2010@gmail.com (H. Hardinsyah), trina_tallei@unsrat.ac.id (T.E. Tallei), apollinaire_tsopmo@carleton.ca (A. Tsopmo), sonradu@gmail.com (S. Radu), edwin.hadinata@yahoo.com (E. Hadinata), bongleekim@khu.ac.kr (B. Kim), rosy@ufsj.edu.br (R.I.M.A. Ribeiro), rony@usu.ac.id (R.A. Syahputra).

https://doi.org/10.1016/j.jafr.2024.101362
Received 10 January 2024; Received in revised form 9 August 2024; Accepted 14 August 2024
Available online 20 August 2024

1. Introduction

Cancer is a non-communicable disease caused by abnormal cell proliferation in benign or malignant tissues. Cancer develops as a result of abnormal activation of oncogenes or deactivation of tumor suppressor genes, both of which disrupt the normal cell cycle [1–3]. Breast cancer has the highest prevalence and mortality rate in women, followed by cervical and ovarian cancer [4]. According to Global Cancer Incidence, Mortality, and Prevalence (GLOBOCAN) data, an estimated 7.8 million people worldwide will be diagnosed with breast cancer by the end of 2020 [5], new cases of breast cancer in Indonesia reached 68,858 (16.6 %) out of a total of 396,914 new cases of breast cancer, and the number of deaths has exceeded 22,000 [6]. Advanced stage breast cancer is often diagnosed too late due to negligence in conducting clinical and self-examination [7]. Advanced breast cancer and local metastases have a poor prognosis, with an average survival rate of less than 5 years. Furthermore, 10 % of newly diagnosed breast cancers progress to the metastatic stage [8].

In Indonesia, treatment of breast cancer includes operative treatment, chemotherapy, and radiation therapy [9]. Chemotherapy has recently become the most common treatment for breast cancer with metastases, but it has the worst side effects, including reduced survival of healthy cells around cancer cells and a tendency to cause necrosis [10]. In addition, the cost of chemotherapy treatment is prohibitive, making this therapy inaccessible to patients with low economic status who are not covered by insurance [11]. New approaches and new anti-tumor compounds need to be constantly sought [12]. Natural resources, such as plants and herbs, offer promising and abundant anticancer potential through receptor inhibitions [13–15]. One of the main receptors to focus on in cancer inhibitor discovery studies is poly (ADP-ribose) polymerase-1 (PARP1) [16,17]. Human epidermal growth factor receptor 2 (HER2) is also a focus of research on candidate substances that can fight breast cancer [8]. In addition, iNOS, an oxidant receptor with a role in radical scavenging and oxidative stressors [13], is another focus of anticancer studies.

PARP1 is a major facilitator of DNA repair and is involved in the tumorigenesis pathway [18]. PARP inhibitors have gained attention recently as rationally-designed therapies for the treatment of some malignancies, especially those associated with dysfunctional DNA repair pathways, including breast cancer [19,20]. Further research on PARP1 as a biomarker for the therapeutic activity of PARP inhibitor-based therapies is needed. In this context, *in vitro* studies on breast cancer cells using the MCF-7 cell line are of value in the search for evidence-based breast cancer inhibitor agents, both *in silico* and *in vitro* [19,20].

Eleutherine bulbosa (Mill.) Urb., known as 'dayak onion' or 'forest onion' in local terminology, is a herbaceous plant in the Iridaceae family that is widely cultivated in Indonesia [21]. *E. bulbosa* can be found throughout Indonesia's sulfur-rich soils, between 600 and 2000 m above sea level on the island of Borneo [22]. Studies by various researchers have revealed the antioxidant and cytotoxic potential of the bioactive constituents of *E. bulbosa* [21]. However, current knowledge of the secondary metabolite profiles of *E. bulbosa* bulb extracts is lacking. Preferably, studies would begin with elucidation and full characterization of metabolite profiles, and *in silico* or docking studies, before *in vitro* studies on specific compounds and anticancer mechanisms. Until now there have been no *in vitro* studies assessing the anticancer effects of *E. bulbosa* in breast cancer with the MCF-7 cell line.

Therefore, this study aims to determine the phytochemical profile of *E. bulbosa* bulb ethanolic extract (EBE) and determine the anticancer activity of its constituents through a pharmacoinformatics approach via *in silico* studies simulating molecular docking, network pharmacology and inhibition of PARP1, HER2 and iNOS receptors. *In vitro* studies on MCF-7 breast cancer cells are also conducted to help determine mechanisms of action and the LD_{50} concentration of EBE. The exploration of new metabolites and bioactive substances for breast cancer therapy is of great interest in the nutraceutical and pharmaceutical industries, and this study will complement other functional anticancer food findings.

2. Materials and methods

2.1. Apparatus and materials

The materials and apparatus used in this study are listed according to the stages of research, including cleaning, drying, determining metabolite profiles, and testing *in silico* and *in vitro*. Apparatus included a drying oven (Memmert Incubator IN55, Schwabach, Germany), rotary evaporator (Merck KGaA, Darmstadt, Germany), blender (CosmosBlender; Tangerang, Indonesia), binocular microscope, spectrophotometer (SmartSpec Plus, Bio-Rad Laboratories. Inc, USA), and a temperature functional centrifuge (Eppendorf, Hamburg, Germany).

Materials used in this study included 96 % ethanol, acetonitrile, methanol, formic acid, trypsin-ethylenediaminetetraacetic acid solution, MCF-7 and MCF-10A, potassium persulfate, sodium chloride, ABTS, mitoxantrone and doxorubicin (Sigma-Aldrich, Darmstadt, Germany); Dulbecco's Modified Eagle Medium (DMEM), Bovine Serum Albumin (BSA), penicillin and streptomycin antibiotics (Thermo Fisher Scientific, USA); DPPH (BioVision, Milpitas, CA, USA); Δ^5-avenasterol or avenasterol (Merck KGaA, Darmstadt, Germany); and TGF-β1, HER2 and p-Akt (Elabscience, Wuhan, China).

Samples of *E. bulbosa* were obtained online, botanical identification and authentication were carried out at the Biochemistry and Biomolecular Laboratory of the Faculty of Medicine, Universitas Brawijaya, Indonesia, and data were matched against taxonomy ID 1210469 (NCBI: txid1210469) of the National Center for Biotechnology Information (NCBI) database. All methods in this research are derived from applicable guidelines and regulations for *in vitro* and plant studies, and the authors confirm that sample collection was approved by the local authorities and complies guidelines.

2.2. E. bulbosa bulb extract (EBE) preparation

E. bulbosa bulb samples were cleaned with distilled water and dehydrated in an oven at 50 °C for 72 h. Sample size reduction was carried out using a blender to provide a coarse simplicia powder. *E. bulbosa* bulb simplicia powder (200 g) was macerated using of 96 % ethanol (2 L) for 72 h with occasional shaking and the mixture was filtered, the filtrate was separated and maceration was repeated for triplicates. The combined filtrates were concentrated using a rotatory evaporator at 70 °C to produce a thick extract of *E. bulbosa* (EBE), which was stored in aluminum foil for use in follow-up tests. This extraction method refers to similar published studies [23].

2.3. Determination of phytochemical profile via untargeted metabolomic profiling

Metabolomic profiling analysis and compound identification was carried out with reference to similar research protocols [24]. After accurately weighing each sample (50 mg) into a tube, 800 μL of 80 % methanol was added, and the mixture was vortexed for 90 s at 4 °C before being sonicated for 30 min. Then, samples were stored at −40 °C for 1 h, vortexed for 30 s, held for 30 min, and centrifuged at the speed of 12,000 rpm for 15 min at 4 °C. Ultimately, a vial containing 200 μL of supernatant was used for LC-MS analysis. Ultra-performance liquid chromatography-tandem mass spectrometry (UPLC-MS/MS) was performed using an Ultimate 3000LC combined with Q Exactive MS (Thermo Fisher, Waltham, USA) with electrospray ionization mass spectrometry (ESI-MS) and an ACQUITY UPLC HSS T3 column (100 × 2.1 mm, 1.8 μm). The mobile phase consisted of solvent A (0.05 % formic acid-water) and solvent B (acetonitrile) with gradient elution (0–1.0 min, 95 % A; 1.0–12.0 min, 95-5% A; 12.0–13.5 min, 5 % A; 13.5–13.6 min, 5–95 % A; 13.6–16.0 min, 95 % A). The flow rate in the

mobile phase was 0.3 mL/min. The sample manager temperature was set at 4 °C, while the column temperature was kept at 40 °C. 40 μL was the injection volume of the sample. The following were the MS parameters in both the negative (ESI−) and positive (ESI+) ion modes. ESI+: capillary temperature of 350 °C, spray voltage of 3.0 KV, casing gas flow rate of 45 arb, aux gas flow rate of 15 arb, sweep gas flow rate of 1 arb, and RF S-lens rate of 30 %. ESI−: capillary temperature of 350 °C; spray voltage of 3.2 KV; casing gas flow rate of 45 arb; aux gas flow rate of 15 arb; sweep gas flow rate of 1 arb. And RF S-lens rate of 60 %.

2.4. In silico study

2.4.1. Prediction of bioactive compound activities and drug likenesses

The compounds isolated from EBE underwent bioactivity analysis utilizing the WAY2DRUG PASS prediction tool (http://www.pharmaexpert.ru/passonline/predict.php, accessed on February 20, 2024), which focuses on cancer treatment, particularly breast cancer, employing SAR analysis to juxtapose input compounds against known ones with specific efficacy [25]. The Pa value (probability of activity) derived from this tool denotes the predicted potency of the compound tested. A Pa exceeding 0.4 suggests substantial potential as an anticancer agent, indicative of similarity to compounds within the database. To ensure accuracy, Pa values > 0.4 were considered in this study, given that higher values correlate with enhanced predictive precision. Additionally, drug likeness, gauging critical pharmacokinetic parameters vital for drug development and toxicity assessment, was evaluated through Lipinski's rule of five (Ro5). This assessment utilized the ADMETLab 2.0 database, employing SMILES notation retrieved from PubChem [26–28]. Detailed compound SMILES notation (https://pubchem.ncbi.nlm.nih.gov, accessed on February 20, 2024) is available in Supplementary Table S1.

2.4.2. Protein target identification and analysis

Target analysis was performed for EBE by putting the SMILES notation for each identified element of EBE into the SuperPred target analysis program (https://prediction.charite.de/, accessed February 20, 2024). For the SuperPred model, the cut-off values for accuracy and probability were chosen at 80 % [29,30]. These genes and proteins were extracted from the Open Targets database (http://www.opentargets.org/), which was retrieved on February 20, 2024, and is linked to breast cancer. A Venn diagram was then used to map the intersection between targets connected to diseases and targets related to EBE. The DAVID website (https://david.ncifcrf.gov/, accessed on February 20, 2024) was used to annotate EBE targets, with an emphasis on biological processes and Kyoto Encyclopedia of Genes and Genomes (KEGG) pathways [31].

2.4.3. Network pharmacology analysis

The investigation into the interplay among target proteins extracted from EBE and their implication in breast cancer was conducted utilizing the STRING database (Version 12.0), a tool designed for the retrieval of interacting genes or proteins [32]. The inquiry encompassed EBE target proteins alongside proteins intersecting with breast cancer, including notable entities such as HIF1A and chlordecone reductase receptors recognized for their close association with breast cancer incidence. Within the STRING database analysis, Homo sapiens (human) was specified as the organism, and interactions were confined to those with a confidence score threshold exceeding 0.4 to ensure robustness. Subsequently, data outputted in TSV format underwent extraction for comprehensive scrutiny employing CytoScape Version 3.10.1. This analysis delved into network intricacies, probing key parameters like degree, betweenness centrality, and closeness centrality among receptors [33].

2.4.4. Molecular docking simulation

ChemDraw Ultra (version 12.0), AutoDock (version 4.2) and BIOVIA Discovery software (version 20.1) were used, and the Protein Data Bank website (https://www.rcsb.org, accessed on May 2, 2023) and the PubChem structure database (https://pubchem.ncbi.nlm.nih.gov, accessed on May 2, 2023) were accessed in the study. All molecular docking simulation protocols refer to published research [34–36]. The X-ray crystallographic structure of human poly(ADP-ribose) polymerase-1 (PARP-1) with A927929, HER2, and iNOS was obtained from the RCSB protein databank with PDB IDs 4UND, 3PP0, and 3E7G, respectively. The crystal structure of all three receptor proteins was prepared by setting up a protein module in Discovery Studio 2.5 to remove crystalline water, prototype the protein structure, and use chemistry in Harvard macromolecular mechanics (CHARMM) force fields. The binding site of the PARP-1 protein was determined by the volume and location of the co-crystallized compound, A927929. Irregular amino acid prediction of receptor proteins was performed by PONDR-Fit.

Redocking serves as a crucial molecular docking validation strategy, whereby the original ligand is transposed onto the target pocket utilizing specific grid coordinates, facilitated by AutoDock. Subsequent to the redocking process, the ligand's positional root-mean-square deviation (RMSD) ideally should not exceed 2.0 Å. Grid and docking parameters were meticulously tailored based on the outcomes derived from docking validation experiments. The resultant data were systematically documented within.dlg files corresponding to each finalized structure of the docking conformation. Evaluation of ligand-receptor interactions was conducted utilizing Discovery Studio 2016, enabling comprehensive analysis and interpretation.

2.5. Antioxidant activity against ABTS and DPPH

The assessment of antioxidant activity entailed the evaluation of radical scavenging potential using 2,2-diphenyl-1-picrylhydrazil (DPPH), as per the methodologies outlined by Hayes et al. [35] and Sabrina et al. [35,37,37]. EBE samples at concentrations of 25, 50, 75, 100, and 125 μg/mL were introduced into test vials containing 3 mL of the DPPH reagent. The resultant mixture was allowed to equilibrate at room temperature for 30 min, and alterations in DPPH concentration were monitored at an absorption wavelength of 517 nm. The scavenging activity against 2,2′-azino-bis(3-ethylbenzothiazoline-6-sulfonic acid) or diammonium salt radical cations (ABTS) was determined following established protocols [35,37]. Specifically, a mixture of potassium persulfate ($K_2S_2O_8$, 2.4 mM) and ABTS (7 mM) was prepared in a 1:1 ratio, shielded from light using aluminum foil, and left to react in the dark at 22 °C for 14 h. This resultant mixture was diluted to generate a working solution with an absorption of 0.706 at 734 nm (e.g., 1 mL of stock solution plus 60 mL of EtOH). A fresh working solution was prepared for each analysis. The EBE sample, stored at concentrations of 25, 50, 75, 100, and 125 μg/mL, was diluted with the ABTS working solution (1 mL), and absorbance was measured after 7 min at 734 nm. The inhibition percentages of DPPH and ABTS were quantified using the following formula:

$$\textbf{Inhibition Activity}\ (\%) = \left[\frac{\mathbf{A0} - \mathbf{A1}}{\mathbf{A0}}\right] \times \mathbf{100\%} \quad (1)$$

where A0 is the blank absorption, and A1 represents the standard or sample absorption.

2.6. In vitro study on cancer cell lines

Universitas Brawijaya's Faculty of Medicine's Biochemistry and Biomolecular Laboratory provided the human breast cancer cells (MCF-7 cell line) and normal breast epithelial cells (MCF-10A cell line). (Malang, Indonesia). In 96-well plates with DMEM, 10 % FBS, and 1 % antibiotic (100 UI/ml penicillin and 100 μl/ml streptomycin), MCF-7 and MCF-10A cells were cultivated. The cultivated cells were placed in an incubator with 5 % CO_2 at 37 °C once they had attained 80 % density. A solution of trypsin-ethylenediaminetetraacetic acid (tryp-sin-

EDTA; Thermo Fisher Scientific, USA) was used to harvest cells on a regular basis.

2.6.1. TGF-β1, p-Akt, HER2 and miR-29a-3p expressions

The *in vitro* assessment of TGF-β1, p-Akt, and HER2 expressions adhered to the protocols provided by respective kit manufacturers (E-AB-33090, Elabscience for TGF-β1; Phospho-AKT Ser473 Kit, Wuhan, China; Elabscience for HER2) and established experimental standards. To detect TGF-β1, HER2, and p-Akt while preventing nonspecific binding, a polyvinylidene difluoride membrane was pre-treated with a blocking solution containing 5 % skimmed dry milk in Tris-Tween saline buffer (T-TBS) containing 0.1 % Tween 20, 20 mmol/L Tris-HCl, 0.138 mol/L NaCl, at a pH of 7.4. Phosphorylated forms of TGF-β1, HER2, and p-Akt were discerned using a blocking solution comprising 5 % albumin (BSA) in T-TBS. This approach facilitated the detection of phosphorylated TGF-β1 and p-Akt. Assessment of TGF-β1, HER2, and p-Akt expression involved membrane exposure to primary antibodies, followed by peroxidase-linked secondary antibodies. Both primary and secondary antibodies were appropriately diluted in 5 % BSA/T-TBS. This meticulous antibody-based methodology aimed at elucidating TGF-β1, HER2, and p-Akt expression while ensuring assay precision through antibody dilution and optimal incubation conditions.

Experimental procedures involved seeding 5000 MCF-7 cells per well at 100 μL/well and treating them with varying concentrations of EBE (0, 100, 200, 300, 400, and 500 μg/mL) for 24 h. Data analysis determined the percentage value relative to the control group, comprising cells untreated or treated with 0 μg/mL EBE. Optical density (OD) measurements at 665 nm and 620 nm wavelengths were conducted using a spectrophotometer for this assessment.

For the MCF-7 cell line, total RNA extraction followed the manufacturer's TRIzol reagent protocol (Invitrogen Life Technologies, USA) and quantification at 260 nm absorption wavelength, performed in triplicate. The cDNA synthesis from 2 μg of total RNA utilized the miScript II RT Kit (QIAGEN, Germany) with stem-loop RT primers for miRNA reverse transcription. The synthesized cDNA was employed to detect miR-29a-3p expression in MCF-7 cells. Quantitative real-time PCR (QRT-PCR) gene detection utilized FastStart Essential DNA Green Master (Roche, USA) following the manufacturer's instructions, with data analyzed using 2-ΔΔCt. Primer sequences for $_{Q}$RT-PCR were as follows: forward primer AGCACCAUCUGAAAUCGGUUA and universal primer GTGCAGGGTCCGAGGT.

2.6.2. MTT assay

The MTT technique was used to conduct the cytotoxicity experiments on the breast cancer cell line MCF-7 and the normal breast epithelial cell line MCF-10A in accordance with the [10]. During a 24-h period, MCF-7 and MCF-10A cells were cultured in 96-well plates and treated with avenasterol and EBE at doses of 0, 100, 200, 300, 400, and 500 μg/mL. Mitoxantrone and doxorubicin were applied as positive controls according to comparable studies [10]. Avenasterol has the best docking value for validation of *in vitro* tests on the cell lines. However, due to limited funds, this test could not be carried out for the other nine identified EBE constituents. In addition, determination of the dose refers to a previous study in which EBE has a reported LD_{50} in the range 100–250 μg/mL against T47D cancer cells [38]. Lower and upper limits of 0 and 500 μg/mL were chosen to determine the effectiveness of the dose. EBE and mitoxantrone (positive control) were added and incubated for 24 h. The cells were isolated with 1X PBS liquid and incubated with 100 μl MTT 0.5 mg/ml at 37 °C. After 30 min, 100 μL of DMEM stopper reagent was added to each well plate. Absorbance was measured at a wavelength of 550 nm using a microplate reader. To minimize the risk of bias, three triple trials were performed for each treatment group. The eligible cells are presented as percentages with the formula:

$$\textbf{Percentage of Living Cells or Viability}\ (\%) = \frac{\mathbf{A} - \mathbf{B}}{\mathbf{C} - \mathbf{B}} \quad (2)$$

where A is the cell absorbance with treatment, B is the absorbance of blank samples, and C is the control cell absorbance.

2.7. Data analytics and management

Data analysis was performed using GraphPad Prism Premium 10 (GraphPad Software, Inc., CA, USA). The data distribution is assessed using the Shapiro-Wilk test. To determine the average difference between treatment groups, a one-way ANOVA test was run if the data were normally distributed (significance <0.05). In all other cases, the Kruskal-Wallis test was used. The LD_{50} for MCF-7 cancer cells, and antioxidant activity towards ABTS and DPPH, were analyzed using GraphPad non-linear regression package (log(inhibitor) vs. normalized response – variable slope); and for the significance values (95 %, CI) for TGF-β1, HER2m miR-29a-3p, and PI3K/AKT expressions through one-way ANOVA tests, and for ABTS and DPPH through two-way ANOVA tests.

3. Results

3.1. Compounds in E. bulbosa extract (EBE)

The total ions and peaks observed in EBE, their elution time, and relative abundance via UPLC-ESI-MS/MS analysis are shown in Fig. 1. The observed compounds were automatically identified through the mzCloud MS/MS Library, and 10 molecules were found to have a match of >99 %. mzCloud database criteria and data are presented in Table 1. The total ion chromatogram (TIC) uses mass spectrometry (MS) parameters in negative ion mode (ESI−, Fig. 1A) and positive ion mode (ESI+, Fig. 1B).

Calculated molecular weights, molecular formulas, and retention times for compounds identified from non-targeted metabolomics profiling via UPLC-ESI-MS/MS are summarized in Table 1. Subsequently, the 10 compounds were applied as ligands to simulate molecular docking. The chemical structures of the EBE metabolites can be found in Supplementary File Table S2.

3.2. Pa score, drug likeness and network pharmacology analysis

Table 2 examines the anticancer potential of compounds (C1–C10) identified in EBE using a detailed structure-activity relationship (SAR) analysis. The investigation includes probable activity (Pa) score and drug likeness evaluations within the framework of network pharmacology. The table carefully compares the compounds' effectiveness as HIF1A expression and chlordecone reductase inhibitors based on the strict criteria established by the Lipinski, Pfizer, and GSK guidelines for medication similarity. The findings demonstrate a range of drug-like qualities and inhibitory abilities, with compounds C1-C4 and C9 demonstrating the best characteristics in all respects. The approval and rejection of C5 and C8 based on various criteria demonstrate the delicate equilibrium between molecular characteristics and potential therapeutic effectiveness. However, all compounds are suitable for further testing in network pharmacology or protein-protein interactions (PPI).

Fig. 2 illustrates the connections between EBE and breast cancer at a molecular level. The Venn diagram in Fig. 2A shows the common molecular targets between EBE constituents and breast cancer-associated genes, indicating potential targets for EBE's therapeutic effects. The PPI network diagrams (Fig. 2B, C, and 2D) illustrate the network of interactions between the proteins. The network diagrams are organized to represent the intensity and specificity of connections, offering insights into how EBE constituents function together on breast cancer pathways. Fig. 2E displays the enriched gene ontology of biological processes among EBE targets, with a clear graphical depiction of the fold enrichment and accompanying false discovery rate (FDR) values. The bar graph highlights the pathways most affected, including those related to

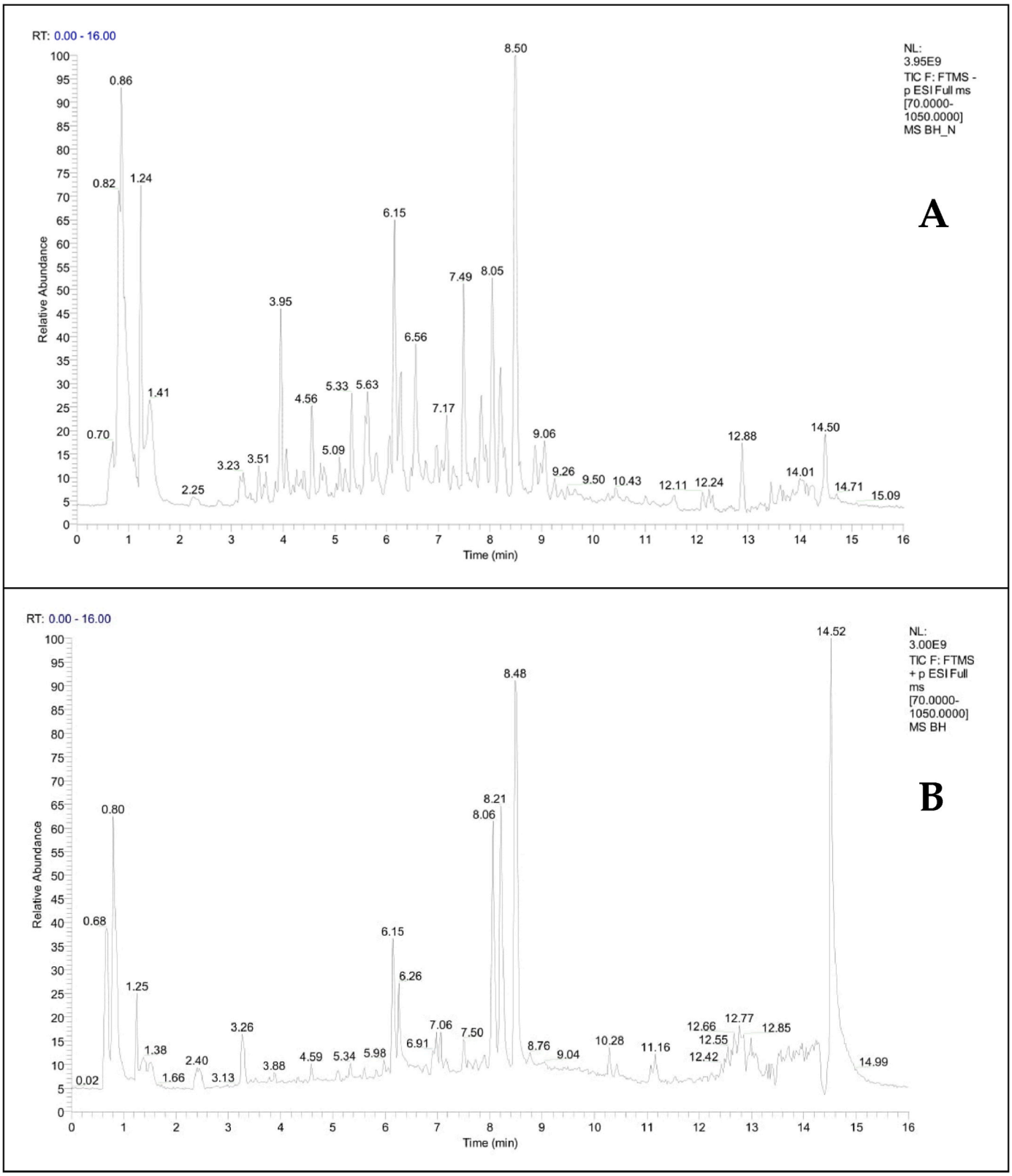

Fig. 1. Total ion chromatogram (TIC) obtained from EBE: (A) TIC in ESI- mode; and (B) TIC in ESI + mode. NL: Neutral loss; FTMS: Fourier transform mass spectrometry.

endocrine resistance and signaling pathways in cancer pathophysiology. This provides a promising outlook for identifying potential biomarkers and therapeutic targets for use of EBE in breast cancer treatment.

Table 3 provides an examination of the main proteins (ERBB2/HER2, PARP1, and NOS2/iNOS) involved in the network of protein-protein interactions (PPI) that play a crucial role in the molecular pathogenesis of breast cancer. The table indicates the importance of a protein in crucial signaling pathways using metrics including degree, betweenness

Table 1
Compounds profile observed in *E. bulbosa* via UPLC-ESI-MS/MS analysis.

Compound	No	Molecular formula	RT (Min)	*m/z*	Molecular weight	PubChem ID
Eleutherol	C1	$C_{14}H_{12}O_4$	8.51	243.0659	244.0731	120697
Genistein	C2	$C_{15}H_{10}O_5$	7.842	269.0451	270.0524	5280961
Luteolin	C3	$C_{15}H_{10}O_6$	7.69	285.0403	286.0476	5280445
Quercetin	C4	$C_{15}H_{10}O_7$	5.676	299.0195	300.0267	5280343
Kaempferol-7-O-glucoside	C5	$C_{21}H_{20}O_{11}$	4.084	447.0926	448.1000	5480982
Elaeokanine C	C6	$C_{12}H_{21}NO_2$	11.249	212.1643	211.1570	442855
Eleutherin	C7	$C_{16}H_{16}O_4$	8.204	273.1116	272.1043	10166
Eicosapentaenoic acid	C8	$C_{20}H_{30}O_2$	9.981	303.2314	302.2241	446284
Tangeritin	C9	$C_{20}H_{20}O_7$	4.155	373.1275	372.1203	68077
Avenasterol	C10	$C_{29}H_{48}O$	13.434	413.3772	412.3699	12795736

Table 2
The evaluation of EBE potential anticancer activity based on structure–activity relationship (SAR) predictions, Pa score, and drug likeness for network pharmacology analysis.

Compounds	Pa score *		Drug likeness **		
	HIF1A expression inhibitor	Chlordecone reductase inhibitor	Lipinski rule	Pfizer rule	GSK
C1	0.85	0.66	Accepted	Accepted	Accepted
C2	0.93	0.92	Accepted	Accepted	Accepted
C3	0.96	0.97	Accepted	Accepted	Accepted
C4	0.96	0.49	Accepted	Accepted	Accepted
C5	0.92	0.87	Rejected	Accepted	Rejected
C6	0.25	0.24	Accepted	Accepted	Accepted
C7	0.54	0.55	Accepted	Accepted	Accepted
C8	0.26	0.83	Accepted	Rejected	Rejected
C9	0.94	0.95	Accepted	Accepted	Accepted
C10	0.35	NA	Accepted	Rejected	Rejected

NA: Not applicable or not found.

centrality, closeness centrality, and an overall score. It highlights the substantial impact of ERBB2/HER2 on the HER2-Akt signaling axis, which is intensified by high levels of HER2 expression, and its impacts on the PIK3CA and MAPK signaling pathways. Researchers have focused on PARP1 and NOS2/iNOS because they play important roles in controlling the TGF-β and nitric oxide signaling pathways. This shows how these proteins interact with each other and how they affect the progression of cancer by modulating cellular processes. Therefore, based on the results of this PPI analysis, the three receptors (HER2, iNOS, PARP1) were selected to continue with molecular docking simulations.

3.3. Molecular docking approach reveals anti-cancer potency of EBE metabolites

Before the 10 EBE constituents (Table 1) proceed to molecular docking simulation (pharmacoinformatics approach), to avoid bias in *in silico* results, each selected receptor should be validated through re-docking tests with their native ligands. Validation test results are shown in Table 4, revealing that the molecular docking protocol performed in this study is valid (root mean square deviation, RMSD <2 Å). The RMSD values provide a nuanced and detailed view of the level of accuracy of docking predictions. In a historical context, it is widely accepted that an RMSD value lower than 2 Å serves as an indicator of precise ligand placement. The validation findings reported in this study consistently demonstrated values below the established threshold. Specifically, the HER2 protein exhibited a measurement of 0.621 Å, the iNOS protein 1.789 Å, and the PARP1 protein 0.854 Å. The very low RMSD observed for HER2 serves to highlight the high level of accuracy with which the compounds were able to align with the binding region of the protein. This finding provides further confirmation of the reliability of the *in silico* evaluations.

Additionally, it should be noted that the validation techniques used here may be utilized as a model for comparable studies. The integration of RMSD values, ΔG measurements, and clustering patterns provides a comprehensive validation framework that guarantees a rigorous verification procedure including precision, energy dynamics, and coherence. The validation data obtained from this work serves to strengthen the accuracy and dependability of the docking predictions conducted for the drugs targeting HER2, iNOS, and PARP1. The results of this study not only confirm the immediate outcomes but also emphasize the wider significance of such validation, ranging from the improvement of drug development procedures to the expedited translation of computational predictions into clinical applications.

The results of molecular docking simulations show that the EBE constituents have the potential to be breast cancer inhibitors by targeting PARP1/HER2/iNOS (Table 5). In the HER2 receptor, all compounds observed in EBE have a more potent binding affinity (ΔG) than the control drug doxorubicin (ΔG -5.17 kcal/mol) (Table 5). In line with the results on HER2, 9 of the 10 compounds had a more potent binding affinity than the control *S*-ibuprofen in inhibiting the iNOS receptor (Table 5). However, at the PARP1 receptor, only the substance avenasterol (ΔG -9.17 kcal/mol) has a more potent binding affinity than the control drug talazoparib (ΔG -8.97 kcal/mol). Hence, avenasterol was revealed to be the crucial substance in EBE with activity in inhibiting all three selected receptors that cause cancer.

In addition to the potential binding affinity, the pattern of amino acid interactions shows that EBE constituents, especially avenasterol, can bind to selected receptor binding sites (Table 6). Therefore, binding of these compounds to HER2 and PARP1 is suspected to induce apoptosis in target cancer cells. A complete visualization of the amino acid interactions of EBE metabolites against HER2, iNOS, and PARP1 can be found in Supplementary File Table S3.

3.4. Anti-oxidative ability of EBE

Given the role of free radicals in the development of cancer, testing the antioxidant activity of potential anticancer agents is important in the discovery of new bioactive compounds. In this study, the anti-oxidative activities of EBE and avenasterol were assessed through their radical scavenging of ABTS and DPPH (Fig. 3). Based on the EC_{50} values, for ABTS free radical scavenging, the EBE value is smaller than the Trolox control (EC_{50} EBE avenasterol < EBE < Trolox) (Fig. 3A). Similarly, in the DPPH inhibitory activity test, the EC_{50} values for EBE and avenasterol were smaller than that for the Trolox control (Fig. 3B). Hence, synergistic antioxidant properties were demonstrated for EBE in *in silico* molecular docking. Certain compounds in Table 5, especially avenasterol, can inhibit iNOS, reactive oxygen and nitrogen metabolite-metabolizing enzymes.

In both free radical scavenging tests, EBE and avenasterol concentrations were not significantly different from the control antioxidant Trolox ($p > 0.05$, except at ABTS concentration 25 μg/mL), indicating similar antioxidant activity in combating free radicals (Fig. 3C and D).

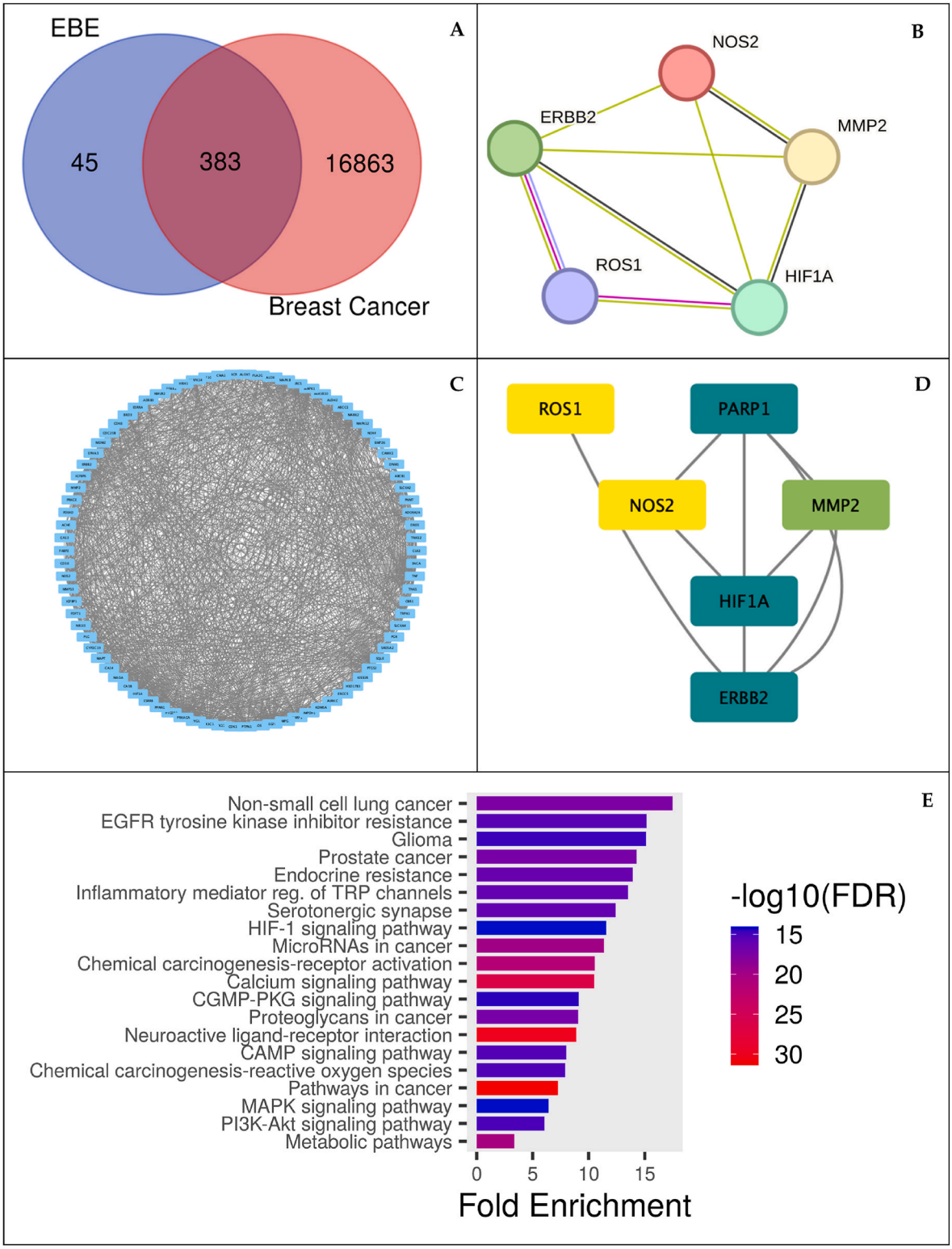

Fig. 2. Network Pharmacology for EBE against breast cancer: (A) Venn diagram showing shared targets between EBE and breast cancer-associated genes; (B,C,D) protein–protein interaction (PPI) of EBE targets in breast cancer; and (E) annotation of gene ontology biological processes for EBE targets (false discovery rate or FDR <0.40).

3.5. EBE suppresses TGF-β, HER2 and PI3K/AKT signaling pathways and modulates miR-29a-3p on MCF-7 cell line

Based on the PPI analysis, the expression of TGF-β/PI3K/AKT/HER2 and miR-29a-3p was assessed in *in vitro* tests. The TGF-β/PI3K/AKT/HER2 signaling pathway and miR-29a-3p modulation was also observed in EBE-treated MCF-7 cancer cells and suppression patterns can be observed in Fig. 4. EBE significantly downregulated TGF-β and HER2 expression compared to the control group in a concentration-dependent manner ($p < 0.0001$, Fig. 4A and C). Furthermore, EBE significantly

Table 3
Results of the top protein–protein interaction (PPI) network analyses.

Name	Degree	Betweenness centrality	Closeness Centrality	Overall score	Pathway
ERBB2 or HER2	4	0.4	0.8333	5.2333	**HER2**–Akt signaling is a product of massive **HER2** expression, **PIK3CA**, **MAPK** signaling pathway
PARP1	4	0.15	0.8333	4.9833	**PARP-1** regulates expression of **TGF-β** receptors and signaling, ROS mediated **TGF-β1**-induced **PARP1** activation, **PI3k/Akt**/FOXO3 pathway
NOS2	2	0.15	0.5555	2.7055	NOS2 - Nitric oxide synthase, inducible; Produces nitric oxide (NO), cytokine-induced **iNOS** promoter activity, the development of cancer via modulating IGF1 mediated **PI3k/Akt**/FOXO3 pathway for **miR-29a-3p** mitigation.

downregulated p-Akt expression in MCF-7 cancer cells, a dose of 500 μg/mL being optimal. This suggests the potential of EBE as an inhibitor of tumorigenesis and breast cancer progression. Interestingly, EBE significantly upregulated tumor suppressor gene miR-29a-3p expression, also in a dose-dependent manner (Fig. 4D). Due to limited resources, the single compound avenasterol has yet to be tested and we have stated this as a limitation of the current research.

3.6. Antiproliferative effect of EBE reveals potential in combating breast cancer

In addition to promising antioxidant and anticancer activity *in silico*, *in vitro* antiproliferation data for EBE and avenasterol reinforce it as a potential drug candidate or functional food for breast cancer treatment (Table 7). The LD_{50} 217.8224 μg/mL for EBE and 50.7880 μg/mL for avenasterol indicate good activities against MCF-7 cells. Interestingly, low cytotoxicity to human epithelial cell line MCF-10A was observed in this study, and EBE can be categorized as a safe functional food candidate (LD_{50} > 1000 μg/mL). Thus, EBE and avenasterol not only present promising biological activities but EBE is also safe for consumption or therapeutic application.

4. Discussion

In the present investigation, our primary objective was to elucidate the binding properties of a diverse range of EBE constituents, both previously reported and newly identified, towards distinct molecular targets including HER2, iNOS, and PARP1 receptors. The successful profiling of EBE metabolites will complement the existing knowledge in the literature, not only providing insight into the molecular interactions between EBE compounds and their specific targets, but also establishing a basis for their potential as therapeutic agents. In pharmaceutical research, particularly in targeted therapeutics, accurately assessing the binding affinity of potential compounds is of utmost importance. These preliminary evaluations serve as a means to filter and select possible pharmaceutical candidates for further examination. Hence, this research represents a crucial milestone in the identification of prospective therapeutic compounds for the treatment of cancers linked to HER2, iNOS,

Table 4
Validation of molecular docking simulation.

No.	Drug Target	PDB ID	Docking site (x; y;z)	Docking area (x; y;z)	RMSD (Å)	ΔG (kcal/mol)	Number in cluster (/100)	Judgment (<2 Å)
1	HER2	3PP0	16.387, 17.394, 26.218,	40 × 40 × 40	0.621	−10.01	39	Valid
2	iNOS	3E7G	55.022, 21.817, 78.677,	40 × 40 × 40	1.789	−6.67	98	Valid
3	PARP1	4UND	24.96, 47.318, 224.969,	42 × 40 × 40	0.854	−9.91	100	Valid

PDB ID: protein data bank identity; RMSD: root mean square deviation.

Table 5
Molecular docking parameter of EBE constituents.

No.	Substance	Number in cluster (/100)			ΔG (kcal/mol)			Ki		
		3PP0	3E7G	4UND	3PP0	3E7G	4UND	3PP0	3E7G	4UND
Control										
1	Doxorubicin	42			−5.17			20.73 uM		
2	*S*-Ibuprofen		33			−4.73			128.28 μM	
3	Talazoparib			80			−8.97			230.91 nM
Compounds in EBE										
1	Avenasterol	98	92	33	−11.26	−8.34	−9.17	1.37 nM	274.78 nM	56.66 nM
2	Eicosapentaenoic acid	27	11	35	−7.67	−3.96	−7.02	375.56 nM	140.60 uM	402.65 nM
3	Elaeokanine C	80	58	47	−6.06	−5.04	−6.87	14.79 uM	137.27 uM	5.30 uM
4	Eleutherin	64	87	100	−8.17	−6.29	−8.54	992.49 nM	23.51 uM	521.51 nM
5	Eleutherol	63	94	78	−6.77	−5.84	−7.13	10.69 uM	50.97 uM	4.92 uM
6	Genistein	81	40	97	−7.16	−5.76	−7.99	5.44 uM	55.39 uM	872.98 nM
7	Kaempferol-7-O-glucoside	30	41	32	−5.99	−6.04	−8.25	10.79 uM	22.32 uM	186.35 nM
8	Luteolin	99	52	96	−7.34	−5.93	−8.53	3.65 uM	23.32 uM	319.03 nM
9	Quercetin	42	54	51	−6.81	−6.02	−8.19	8.84 uM	28.70 uM	498.18 nM
10	Tangeritin	99	76	35	−7.64	−5.4	−6.99	1.42 uM	92.84 uM	6.23 uM

Table 6
Amino acid interaction visualization of avenasterol metabolite against HER2, iNOS, and PARP1.

No.	Substance	Ligand interaction
1	Avenasterol with HER2	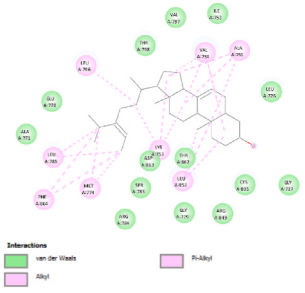
2	Avenasterol with iNOS	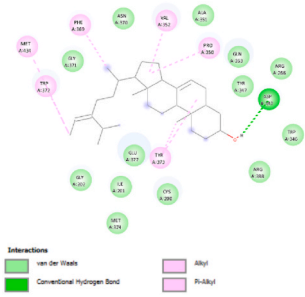
3	Avenasterol with PARP1	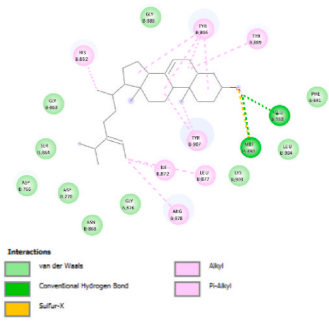

and PARP1, especially breast cancer.

Doxorubicin is a chemotherapeutic drug whose interaction with the protein target HER2 is characterized by a binding energy of −5.17 kcal/mol, concomitant with a Ki value of 20.73 μM. These values provide the standard by which novel compounds may be compared. As an example, avenasterol, a newly identified molecule in EBE, has a notable binding affinity of −11.26 kcal/mol with HER2 and a significantly reduced Ki value of 1.37 nM. The observed disparity underscores the heightened affinity and possible efficacy of avenasterol relative to doxorubicin in relation to this specific target. At the same time, this finding may also imply the possible substitution of doxorubicin, which may induce oxidative and inflammatory conditions [39]. Similar parallels may be established between substances such as eleutherin and luteolin, possibly due to their similar anti-cancer activities of suppressing essential regulatory pathways linked to the development of cancer, inducing oxidative stress, halting the cell cycle, increasing the expression of genes related to apoptosis, and hindering both cell proliferation and angiogenesis in cancer cells [40]. This underscores the significance of identifying molecules exhibiting enhanced binding characteristics. Furthermore, the arrangement of EBE constituents inside the clusters provides information on their coherence and dependability in relation to target interactions. Clusters exhibiting high numbers, such as tangeritin for HER2 and eleutherol for PARP1, suggest a strong and reliable pattern of interaction. The presence of a constant clustering pattern indicates that the molecule forms stable conformations in numerous states, which is crucial for maintaining the efficacy and dependability of treatments.

S-Ibuprofen, serving as an additional control, shows a binding energy of −4.73 kcal/mol with 3PP0 and a Ki value of 128.28 μM. The broad binding landscape becomes clear when comparing it to newly identified molecules eicosapentaenoic acid and elaeokanine C. While elaeokanine C has significantly enhanced binding energy profiles, eicosapentaenoic acid displays a more intricate equilibrium between binding energy and inhibition constants. These differences serve to emphasize the diverse nature of the newly identified chemicals, while also highlighting potential avenues for improvement and focused pharmaceutical research.

Talazoparib, renowned for its potent inhibition of PARP1, has a very high binding affinity of −8.97 kcal/mol, as shown by its Ki value in the nanomolar range. The comparison proves to be enlightening. Compounds like genistein, which has a binding energy of −7.99 kcal/mol and a Ki value of 872.98 nM with 4UND, have competitive characteristics. This observation implies the potential for these compounds to serve as viable replacements or supplementary agents to current PARP1 inhibitors. The use of a comparative framework, when applied to compounds such as kaempferol-7-O-glucoside and quercetin, presents the merits and constraints of these compounds as anti-breast cancer agents in connection to existing pharmaceuticals. The new compounds have considerable potential when compared to existing control compounds, not only demonstrating enhanced binding affinities, but their persistent clustering patterns also suggest the possibility of durable and dependable therapeutic effects. However, although preliminary results are encouraging, more experimental verification is necessary to thoroughly assess the therapeutic capabilities of these molecules.

In vitro, various researchers have assessed the antioxidant and cytotoxic activity of *E. bulbosa* [21]. However, cytotoxicity in breast cancer cells has not been assessed previously, even though breast cancer has the highest prevalence and mortality rate in women, followed by cervical cancer and ovarian cancer. Most of the constituents evaluated in EBE are naphthoquinone derivatives thought to have anti-tumor potential [21]. According to Lestari et al. [41], EBE has anti-leukemia activity at 9.56 ppm (very strong category) and antioxidant activity with an IC_{50} value of 19.694 ppm [41]. Moreover, Kamarudin et al. in 2022 reported that EBE could markedly suppress proliferation of retinoblastoma cancer cells with an LC_{50} value of 15.7 μg/mL [42]. The current research complements the anticancer potential of EBE, in particular against breast cancer, and indicates promising antioxidant activity in fighting free radicals. The antioxidant properties of EBE are thought to contribute strongly to suppressing breast cancer cell proliferation through suppressing TGF-β1, HER2, and PI3K/AKT signaling pathways (Fig. 5). Avenasterol and other metabolites in EBE are thought to suppress or inhibit iNOS, resulting in suppression of PI3K/AKT (Fig. 5). This is in line with a meta-analysis highlighting that consumption of antioxidants such as fucoidan hinders the development and natural spread of tumors [43]. With TGF-β1, iNOS, and HER2 inhibition, this also downregulates smad2 and smad3 which will be followed by downregulation of PTEN and PI3K/AKT signaling pathway, and upregulation of miR-29a-3p expression and pro-apoptotic factors (such as Bax). Hence, EBE can induce anti-proliferation and apoptosis in breast cancer cells (Fig. 5). Thus, the current study provides additional evidence of anticancer activity, especially for breast cancer, through modulations of apoptosis-inducing molecular biomechanisms. Through the inhibition of PARP1 proven in this *in silico* study, EBE appears to play a role in preventing DNA damage caused by PARP1, thus maintaining cells in normal proliferation conditions (Fig. 5). Furthermore, in breast cancer cells, EBE can inhibit PARP1, causing DNA damage and inducing synthetic lethality and cancer cell death (Fig. 5).

Given the promise of EBE as an anticancer agent, further development of EBE products is required to explore their effectiveness and health benefits. To ensure the validity and safety of EBE research development, the drug discovery process must be carried out according to FDA recommendations (Fig. 6).

In a preliminary stage, metabolomics profiling identifies processes or

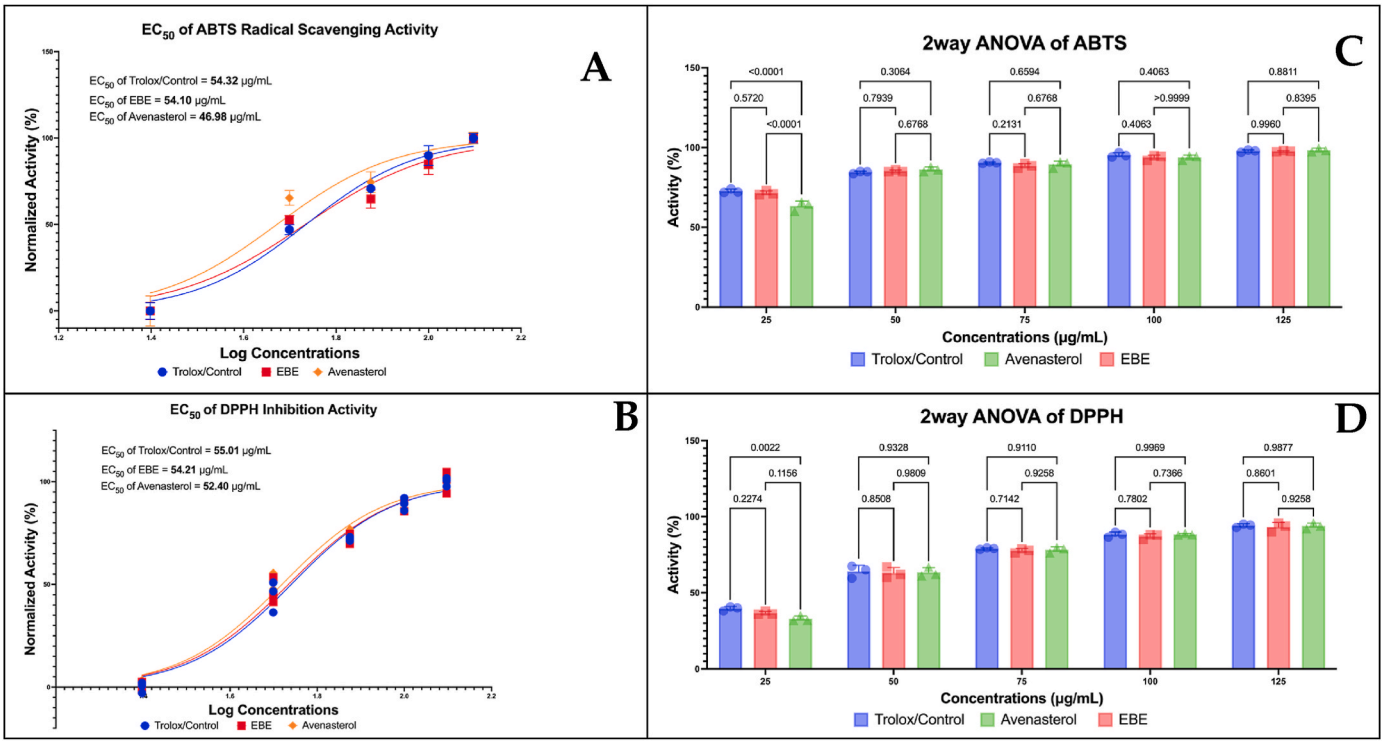

Fig. 3. Antioxidant activity of EBE and avenasterol: (A) EC_{50} ABTS inhibition activity; (B) EC_{50} DPPH inhibition activity; (C) two-way ANOVA of ABTS inhibition activity in gradient concentrations; and (D) two-way ANOVA of DPPH inhibition activity in gradient concentrations.

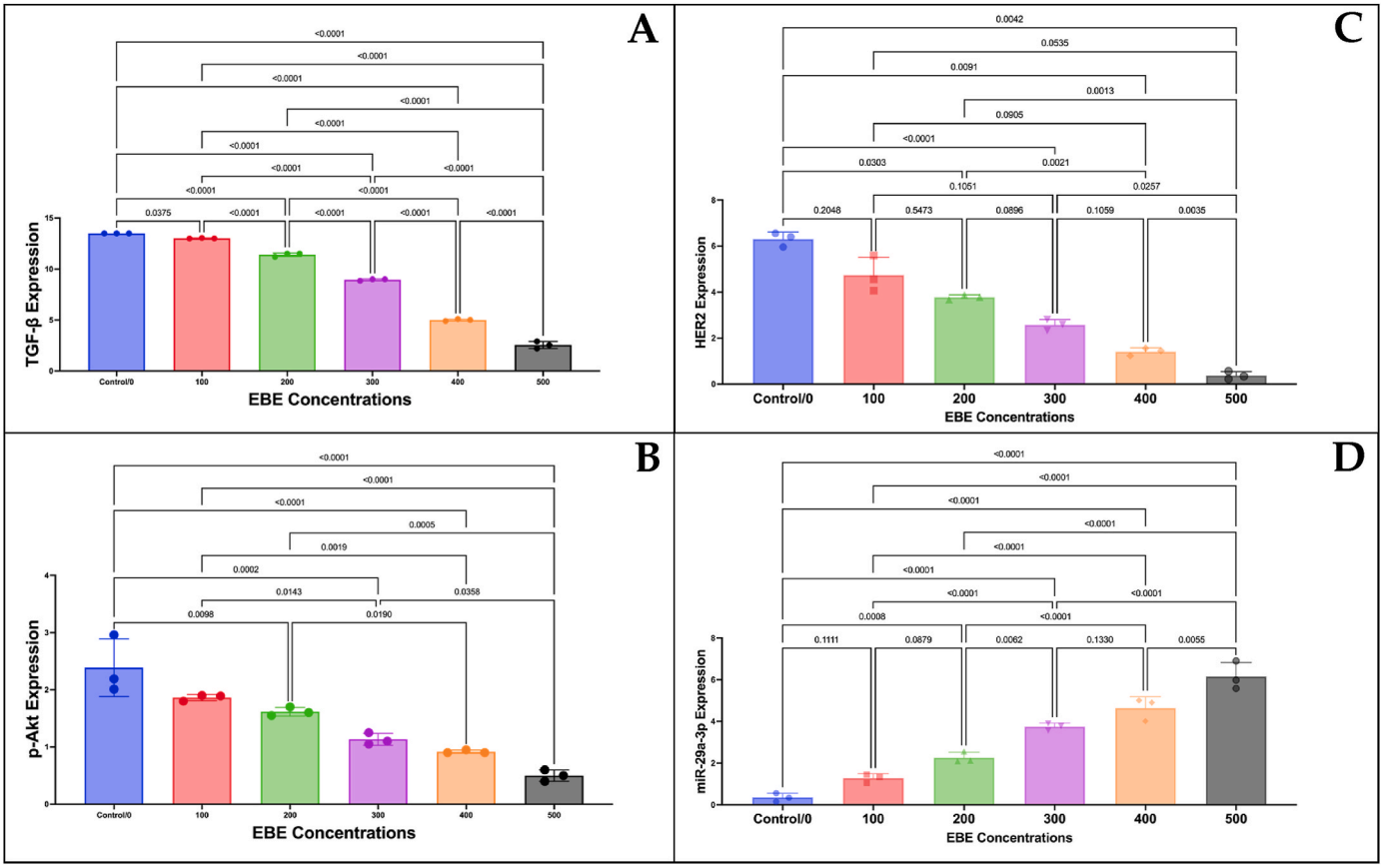

Fig. 4. Suppression of TGF-β1, p-Akt, HER2 and upregulation of miR-29a-3p expressions on MCF-7 cell line by EBE: (A) one-way ANOVA of TGF-β1 suppression by EBE; (B) one-way ANOVA of p-Akt suppression by EBE; (C) one-way ANOVA of HER2 suppression by EBE; and (D) one-way ANOVA of miR-29a-3p upregulation by EBE.

Table 7
LD_{50} values (μg/mL) of EBE on MCF-7 breast cancer and normal (epithelial) cell lines.

No	Samples	Cancer MCF-7	Normal cell MCF-10A
1	EBE	217.8224	1397.5851
2	Avenasterol	50.7880	1025.3455
3	Control M	22.2373	17.8949
4	Control D	6.3555	24.9407

M, mitoxantrone; D, doxorubicin.

target pathways influencing breast cancer and its accompanying diseases. *In silico* network pharmacology and molecular docking simulations have been conducted to identify and screen compounds with potential as drug candidates. Thus, *in silico* studies can validate targets and determine whether EBE constituents can provide therapeutic benefits to breast cancer targets. Preclinical trials are needed to evaluate the therapeutic index and dose using *in vitro* and *in vivo* approaches, and to evaluate pharmacokinetic and pharmacodynamic factors in experimental animals (Fig. 6). Lastly, to ensure efficacy and safety, three phases of clinical trials need to be conducted in breast cancer patients.

The results of the present research highlight the complex nature of the interactions between EBE constituents and three protein-receptor targets HER2, iNOS, and PARP1. The compounds have significant potential as anticancer therapeutic agents due to their capacity to bind to various targets with different affinities. This is advantageous in the treatment of complicated disorders like cancer that need a multifaceted approach. Although preliminary results provide a solid foundation, further investigation should aim to explore the underlying mechanisms that contribute to these associations, elucidating the complex structural dynamics involved. Additionally, this study examines possible synergistic effects of EBE that may be used to enhance the efficacy of therapeutic treatments in breast cancer. In addition, combining *in silico* and *in vitro* studies can provide new evidence-based insights into its anticancer benefits.

This study has certain limitations. Different *E. bulbosa* extracts with

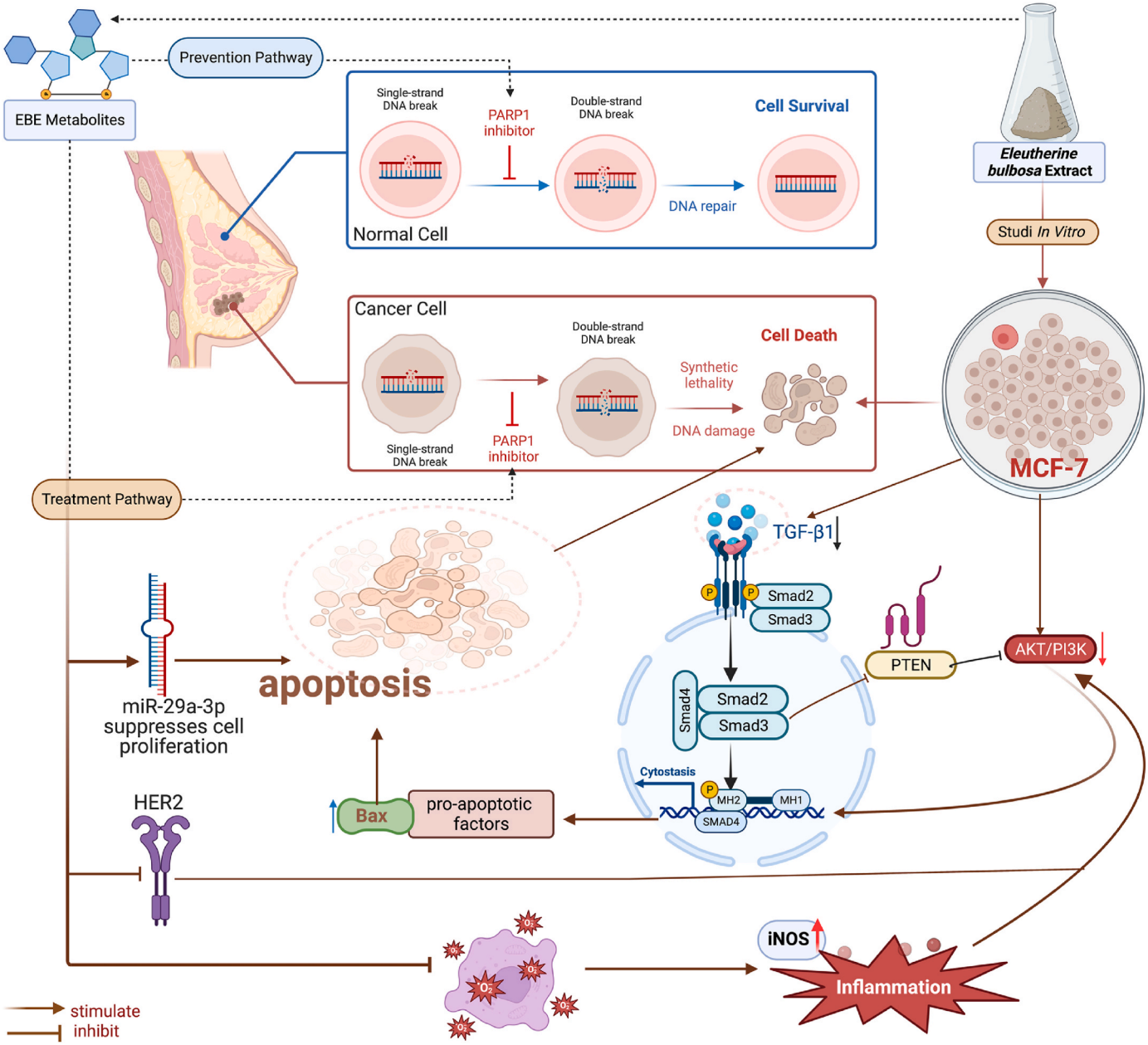

Fig. 5. Possible biomechanism of EBE in modulating breast cancer pathways.

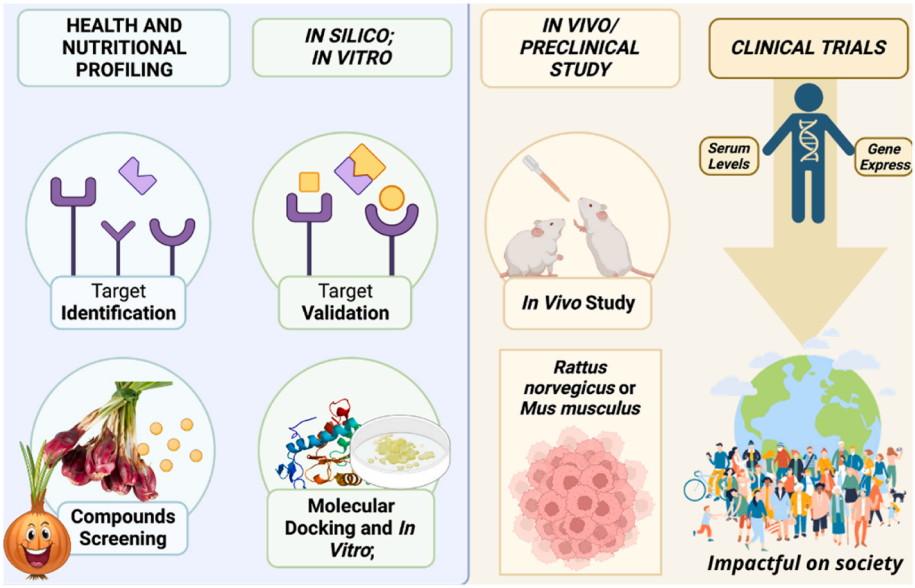

Fig. 6. Current and future prospective studies on EBE. The blue zone is the scope of the present study.

other solvents, and improved methods of isolation of constituents with anticancer activity, are worthy of further investigation. Researchers had resource limitations which prevented testing the single compound avenasterol on the TGF-β1, p-Akt, HER2 and miR-29a-3p expressions. However, it is hoped that testing EBE for TGF-β1, p-Akt, HER2 and miR-29a-3p expressions in MCF-7 provides insight to initiate future research. In this study, validation of avenasterol has been carried out in antioxidant tests and *in vitro* antiproliferative tests. Furthermore, the combination of *in silico* with *in vitro* does not fully represent *in vivo* results or human clinical trials. Therefore, the authors plan further studies to elucidate the anticancer effectiveness of EBE.

This section may be divided by subheadings. It should provide a concise and precise description of the experimental results, their interpretation, as well as the experimental conclusions that can be drawn.

5. Conclusions

This study comprehensively reveals the active constituent profile of *Eleutherine bulbosa* bulb ethanol extract (EBE), identifying especially the compound avenasterol, and its molecular mechanisms as an agent with potential in breast cancer treatment through inhibition of the PARP1/HER2/iNOS proteins. *In vitro* studies on MCF-7 cell lines validated the promising anticancer activity of EBE and avenasterol, showing relatively low cytotoxicity to normal cells, and safety for consumption and therapeutic application. Interestingly, EBE significantly suppressed TGF-β1, HER2 and PI3K/AKT expressions, inducing an apoptotic effect on the MCF-7 cell line. In conclusion, EBE has potential as in breast cancer treatment by downregulating PARP1/HER2/iNOS, and upregulating tumor suppressor miR-29a-3p and TGF-β1/PI3K/AKT/HER2 signaling pathway. *In vitro* cytotoxicity on a MCF-7 cell line suggests promise for development as an advanced functional food product. Importantly, follow-up studies such as *in vivo* animal model experiments and clinical trials with cancer patients are recommended.

Patents

The extraction method with its formulation resulting from the work reported in this article has been registered as a patent (Fahrul Nurkolis is the patent holder) in Indonesia.

Funding

This study was funded by Universitas Sumatera Utara.

Institutional review board statement

Not applicable.

Informed consent statement

Not applicable.

Data availability statement

The datasets presented in this study can be requested from the corresponding author or F.N.

CRediT authorship contribution statement

Fahrul Nurkolis: Writing – review & editing, Writing – original draft, Visualization, Software, Resources, Project administration, Methodology, Investigation, Formal analysis, Data curation, Conceptualization. **Isma Kurniatanty:** Writing – original draft, Visualization, Validation, Methodology, Conceptualization. **Elvan Wiyarta:** Writing – original draft, Formal analysis, Data curation. **Happy Kurnia Permatasari:** Writing – review & editing, Validation, Supervision, Project administration, Methodology, Investigation, Formal analysis. **Nelly Mayulu:** Writing – review & editing, Validation, Resources. **Nurpudji Astuti Taslim:** Writing – review & editing, Validation, Supervision. **Raymond Rubianto Tjandrawinata:** Writing – review & editing, Validation. **Hardinsyah Hardinsyah:** Writing – review & editing. **Trina Ekawati Tallei:** Writing – review & editing. **Apollinaire Tsopmo:** Writing – review & editing. **Son Radu:** Writing – review & editing, Supervision. **Edwin Hadinata:** Writing – review & editing. **Bonglee Kim:** Writing – review & editing, Supervision, Funding acquisition. **Rosy Iara Maciel Azambuja Ribeiro:** Writing – review & editing, Validation. **Rony Abdi Syahputra:** Writing – original draft, Validation, Project administration, Methodology, Investigation, Funding acquisition, Formal analysis.

Declaration of competing interest

The authors declare that they have no known competing financial interests or personal relationships that could have appeared to influence the work reported in this paper.

Data availability

Data will be made available on request.

Acknowledgments

The authors would like to express their thanks to all contributors who have provided input and motivation in conducting the research reported in this article.

Appendix A. Supplementary data

Supplementary data to this article can be found online at https://doi.org/10.1016/j.jafr.2024.101362.

References

[1] M. Herre, J. Cedervall, N. Mackman, A.K. Olsson, NEUTROPHIL EXTRACELLULAR TRAPS IN THE PATHOLOGY OF CANCER AND OTHER INFLAMMATORY DISEASES, 2023.
[2] T. Soussi, K.G. Wiman, TP53: an Oncogene in Disguise, 2015.
[3] L.H. Wang, C.F. Wu, N. Rajasekaran, Y.K. Shin, Loss of Tumor Suppressor Gene Function in Human Cancer: an Overview, 2019.
[4] M. Yi, T. Li, M. Niu, S. Luo, Q. Chu, K. Wu, Epidemiological trends of women's cancers from 1990 to 2019 at the global, regional, and national levels: a population-based study, Biomark. Res. 9 (2021) 1–12, https://doi.org/10.1186/s40364-021-00310-y.
[5] M. Arnold, E. Morgan, H. Rumgay, A. Mafra, D. Singh, M. Laversanne, et al., Current and future burden of breast cancer: global statistics for 2020 and 2040, Breast 66 (2022) 15–23, https://doi.org/10.1016/j.breast.2022.08.010.
[6] D. Gayatri, L. Efremov, R. Mikolajczyk, E.J. Kantelhardt, Quality of life assessment and pain severity in breast cancer patients prior to palliative oncology treatment in Indonesia: a cross-sectional study, Patient Prefer. Adherence 15 (2021) 2017–2026, https://doi.org/10.2147/PPA.S320972.
[7] M. Akram, M. Iqbal, M. Daniyal, A.U. Khan, Awareness and Current Knowledge of Breast Cancer, 2017.
[8] K. Barzaman, S. Moradi-Kalbolandi, A. Hosseinzadeh, M.H. Kazemi, H. Khorramdelazad, E. Safari, et al., Breast Cancer Immunotherapy: Current and Novel Approaches, 2021.
[9] H.K. Permatasari, I.D. Kusuma, E. Mayangsari, Minyak cengkeh (syzygium aromaticum) menginduksi apoptosis pada sel kanker servik HeLa melalui peningkatan kadar protein p53, Jurnal Kedokteran Brawijaya 30 (2019) 185–190, https://doi.org/10.21776/ub.jkb.2019.030.03.4.
[10] F. Nurkolis, N.A. Taslim, F.R. Qhabibi, S. Kang, M. Moon, J. Choi, et al., Ulvophyte green algae *Caulerpa lentillifera*: metabolites profile and antioxidant, anticancer, anti-obesity, and in vitro cytotoxicity properties, Molecules 28 (2023) 1365, https://doi.org/10.3390/MOLECULES28031365, 2023b;28:1365.
[11] F. Nurkolis, F.R. Qhabibi, V.M. Yusuf, S. Bulain, G.N. Praditya, D.G. Lailossa, et al., Anticancer properties of soy-based tempe: a proposed opinion for future meal, Front. Oncol. 12 (2022), https://doi.org/10.3389/fonc.2022.1054399.
[12] Q. Qi, R. Li, H.Y. Li, Y.B. Cao, M. Bai, X.J. Fan, et al., Identification of the anti-tumor activity and mechanisms of nuciferine through a network pharmacology approach, Acta Pharmacol. Sin. 37 (2016) 963–972, https://doi.org/10.1038/aps.2016.53.
[13] R. Gopalakrishnan, A.I. Frolov, L. Knerr, W.J. Drury, E. Valeur, Therapeutic potential of foldamers: from chemical biology tools to drug candidates? J. Med. Chem. 59 (2016) 9599–9621, https://doi.org/10.1021/acs.jmedchem.6b00376.
[14] P. Kaushik, P. Ahlawat, K. Singh, R. Singh, Chemical constituents, pharmacological activities, and uses of common ayurvedic medicinal plants: a future source of new drugs, Advances in Traditional Medicine 23 (2023) 673–714, https://doi.org/10.1007/s13596-021-00621-3.
[15] A.D.R. Nurcahyanti, A. Jap, J. Lady, D. Prismawan, F. Sharopov, R. Daoud, et al., Function of Selected Natural Antidiabetic Compounds with Potential against Cancer via Modulation of the PI3K/AKT/mTOR Cascade, 2021.
[16] N.J. Curtin, C. Szabo, Poly(ADP-ribose) polymerase inhibition: past, present and future (2020).
[17] Y.Q. Wang, P.Y. Wang, Y.T. Wang, G.F. Yang, A. Zhang, Z.H. Miao, An Update on poly(ADP-Ribose)polymerase-1 (PARP-1) Inhibitors: Opportunities and Challenges in Cancer Therapy, 2016.
[18] V. Ossovskaya, I.C. Koo, E.P. Kaldjian, C. Alvares, B.M. Sherman, Upregulation of poly (ADP-Ribose) polymerase-1 (PARP1) in triple-negative breast cancer and other primary human tumor types, Genes and Cancer 1 (2010) 812–821, https://doi.org/10.1177/1947601910383418.
[19] K.M. Frizzell, M.J. Gamble, J.G. Berrocal, T. Zhang, R. Krishnakumar, Y. Cen, et al., Global analysis of transcriptional regulation by poly(ADP-ribose) polymerase-1 and poly(ADP-ribose) glycohydrolase in MCF-7 human breast cancer cells, J. Biol. Chem. 284 (2009) 33926–33938, https://doi.org/10.1074/jbc.M109.023879.
[20] X.W. Meng, B.D. Koh, J.S. Zhang, K.S. Flatten, P.A. Schneider, D.D. Billadeau, et al., Poly(ADP-ribose) polymerase inhibitors sensitize cancer cells to death receptor-mediated apoptosis by enhancing death receptor expression, J. Biol. Chem. 289 (2014) 20543–20558, https://doi.org/10.1074/jbc.M114.549220.
[21] A.A. Kamarudin, N.H. Sayuti, N. Saad, N.A.A. Razak, N.M. Esa, *Eleutherine bulbosa* (Mill.) urb, bulb: Review of the pharmacological activities and its prospects for application (2021).
[22] T. Ieyama, M.D.P.T. Gunawan-Puteri, J. Kawabata, α-Glucosidase inhibitors from the bulb of *Eleutherine americana*, Food Chem. 128 (2011) 308–311, https://doi.org/10.1016/j.foodchem.2011.03.021.
[23] A.A. Kamarudin, Mohd, N. Esa, N. Saad, N.H. Sayuti, N.A. Nor, Heat assisted extraction of phenolic compounds from *Eleutherine bulbosa* (Mill.) bulb and its bioactive profiles using response surface methodology, Ind. Crop. Prod. 144 (2020) 112064, https://doi.org/10.1016/j.indcrop.2019.112064.
[24] H. Simbala, F. Nurkolis, N. Mayulu, L. Rotty, New discovery of covid-19 natural-based potential Antivirus herbal supplement products from pinang yaki (*Areca vestiaria*) extract: a preliminary study by untargeted metabolomic profiling, F1000Research 10 (2022) 1021, https://doi.org/10.12688/f1000research.73758.2.
[25] D.S. Druzhilovskiy, A.V. Rudik, D.A. Filimonov, T.A. Gloriozova, A.A. Lagunin, A. V. Dmitriev, et al., Computational platform Way2Drug: from the prediction of biological activity to drug repurposing, Russ. Chem. Bull. 66 (2017) 1832–1841, https://doi.org/10.1007/s11172-017-1954-x.
[26] P. Banerjee, A.O. Eckert, A.K. Schrey, R. Preissner, ProTox-II: a webserver for the prediction of toxicity of chemicals, Nucleic Acids Res. 46 (2018) W257–W263, https://doi.org/10.1093/nar/gky318.
[27] J. Dong, N.-N. Wang, Z.-J. Yao, L. Zhang, Y. Cheng, D. Ouyang, et al., ADMETlab: a platform for systematic ADMET evaluation based on a comprehensively collected ADMET database, J Cheminform 10 (2018), https://doi.org/10.1186/s13321-018-0283-x.
[28] U. Norinder, C.A.S. Bergström, Prediction of ADMET properties, ChemMedChem 1 (2006) 920–937, https://doi.org/10.1002/cmdc.200600155.
[29] M. Dunkel, S. Günther, J. Ahmed, B. Wittig, R. Preissner, SuperPred: drug classification and target prediction, Nucleic Acids Res. 36 (2008) W55–W59, https://doi.org/10.1093/nar/gkn307.
[30] K. Gallo, A. Goede, U. SuperPred 3.0: drug classification and target prediction—a machine learning approach, AcademicOupCom (2022) n.d.
[31] D. Gfeller, A. Grosdidier, M. Wirth, A. Daina, O. Michielin, V. Zoete, SwissTargetPrediction: a web server for target prediction of bioactive small molecules, Nucleic Acids Res. 42 (2014) W32–W38, https://doi.org/10.1093/nar/gku293.
[32] A. Asadzadeh, N. Ghorbani, K. Dastan, Identification of druggable hub genes and key pathways associated with cervical cancer by protein-protein interaction analysis: an in silico study, Int J Reprod Biomed (Yazd) 21 (2023) 809–818, https://doi.org/10.18502/ijrm.v21i10.14536.
[33] Sun P, Yang Y, Cheng H, Fu S, Liu Y, et al. Integrated analysis of long non-coding RNA expression profiles in glaesserella parasuis-induced meningitis: new insight into pathogenesis. MdpiCom n.d.
[34] K.-C. Chen, M.-F. Sun, C.Y.-C. Chen, In silico investigation of potential PARP-1 inhibitors from traditional Chinese medicine, Evid. base Compl. Alternative Med. 2014 (2014) 917605, https://doi.org/10.1155/2014/917605.
[35] C. Hayes, F. Nurkolis, D.A. Laksemi, S. Chung, M.N. Park, M. Choi, et al., Coffee Silverskin Phytocompounds as a Novel Anti-aging Functional Food: A Pharmacoinformatic Approach Combined with in Vitro Study, 2023.
[36] F. Nurkolis, A.F. Purnomo, D. Alisaputra, W.B. Gunawan, F.R. Qhabibi, W. Park, et al., In silico and in vitro studies reveal a synergistic potential source of novel anti-ageing from two Indonesian green algae, J. Funct.Foods 104 (2023) 105555, https://doi.org/10.1016/j.jff.2023.105555.
[37] N. Sabrina, M. Rizal, F. Nurkolis, H. Hardinsyah, M.J. Tanner, W. Ben Gunawan, et al., Bioactive peptides identification and nutritional status ameliorating properties on malnourished rats of combined eel and soy-based tempe flour, Front. Nutr. 9 (2022) 2196, https://doi.org/10.3389/fnut.2022.963065.
[38] R. Mutiah, F. Choiroh, R. Annisa, A. Listiyana, Combinational effect of *Eleutherine palmifolia* (L.) merr extract and doxorubicin chemotherapy on HeLa cervical cancer cells, AIP Conf. Proc. 2120 (2019) 70001, https://doi.org/10.1063/1.5115718. American Institute of Physics Inc.
[39] O.A. Akinloye, L.A. Sulaimon, O.E. Ogunbiyi, A.E. Odubiyi, A.A. Adewale, M. A. Toriola, et al., Amaranthus spinosus (Spiny Pigweed) methanol leaf extract alleviates oxidative and inflammation induced by doxorubicin in male sprague dawley rats, Advances in Traditional Medicine 23 (2023) 1231–1248, https://doi.org/10.1007/s13596-022-00677-9.
[40] P. Prasher, M. Sharma, S.K. Singh, M. Gulati, D.K. Chellappan, F. Zacconi, et al., Luteolin: a flavonoid with a multifaceted anticancer potential, Cancer Cell Int. 22 (2022) 386, https://doi.org/10.1186/s12935-022-02808-3.

[41] D. Lestari, R. Kartika, E. Marliana, Antioxidant and anticancer activity of *Eleutherine bulbosa* (Mill.) Urb on leukemia cells L1210, J. Phys. Conf. 1277 (2019) 012022, https://doi.org/10.1088/1742-6596/1277/1/012022. IOP Publishing.
[42] A.A. Kamarudin, N.H. Sayuti, N. Saad, N.A.A. Razak, N.M. Esa, Induction of apoptosis by *Eleutherine bulbosa* (Mill.) Urb. bulb extracted under optimised extraction condition on human retinoblastoma cancer cells (WERI-Rb-1), J. Ethnopharmacol. 284 (2022) 114770, https://doi.org/10.1016/j.jep.2021.114770.
[43] L.-M. Cao, Z.-X. Sun, E.C. Makale, G.-K. Du, W.-F. Long, H.-R. Huang, Antitumor activity of fucoidan: a systematic review and meta-analysis, Transl. Cancer Res. 10 (2021) 5390–5405, https://doi.org/10.21037/tcr-21-1733.